UDK 669.14.018.252:539.42:621.785.72
Original scientific article/Izvirni znanstveni članek

ISSN 1580-2949
MTAEC9, 46(5)489(2012)

INFLUENCE OF SEGREGATIONS ON THE FRACTURE TOUGHNESS K_{Ic} OF HIGH-STRENGTH SPRING STEEL

VPLIV IZCEJ NA LOMNO ŽILAVOST K_{Ic} VISOKOTRDNOSTNEGA VZMETNEGA JEKLA

Bojan Senčič[1,2], Vojteh Leskovšek[2,3]

[1]ŠTORE STEEL, d. o. o., Železarska cesta 3, 3220 Štore, Slovenia
[2]Jožef Stefan International Postgraduate School, Jamova 39, 1000 Ljubljana, Slovenia
[3]Institute of Metals and Technology, Lepi pot 11, 1000 Ljubljana, Slovenia
bojan.sencic@store-steel.si

Prejem rokopisa – received: 2012-03-19; sprejem za objavo – accepted for publication: 2012-05-07

The results of this investigation showed that using the proposed method it was possible to draw, for the normally used range of working hardnesses, a tempering diagram (Rockwell-C hardness – fracture toughness K_{Ic} – tempering temperature) for the vacuum-heat-treated high-strength spring-steel grade 51CrV4. Based on measurements of the mechanical properties we have also created a classic tempering diagram, i.e., Tensile strength R_m – Yield stress $R_{p0.2}$ – Elongation A_5/% – Necking Z/% – Tempering temperature, and a tempering diagram, i.e., Hardness HRc – Impact toughness Charpy-V – Tempering temperature. According to these tempering diagrams we can conclude that the investigated spring steel 51CrV4 is suitable for the production of high-strength springs when using the proper heat treatment. Fractographic and metallographic analyses of the K_{Ic} test specimens showed the presence of segregations in the steel. Therefore, we focused on examining the impact of segregations on the fracture toughness K_{Ic}. We found that the widths of the positive segregation bands and the matrix bands between the samples vary considerably. We have also discovered that the number and the width of the segregation bands influence significantly the fracture toughness K_{Ic} due to the presence of bainite in the matrix bands.

Keywords: fracture toughness, segregations, high-strength spring steel, vacuum heat treatment, tempering diagrams, microstructure

Pri opravljenih preiskavah smo želeli ugotoviti, ali lahko standardizirano preizkušanje lomne žilavosti (ASTM E399-90) nadomestimo z nestandardnim postopkom preizkušanja lomne žilavosti s cilindričnim nateznim preizkušancem z zarezo po obodu in utrujenostno razpoko v dnu zareze. Inovativen način preiskav je pokazal, da lahko s predlagano metodo konstruiramo diagram popuščanja (trdota Rockwell-C – lomna žilavost K_{Ic} – temperatura popuščanja) za vakuumsko toplotno obdelano visokotrdnostno vzmetno jeklo. Na osnovi meritev mehanskih lastnosti smo izdelali poleg klasičnega diagrama popuščanja: natezna trdnost R_m – meja plastičnosti $R_{p0.2}$ – raztezek A_5/% – kontrakcija Z/% – temperatura popuščanja, še diagram popuščanja trdota HRc – udarna žilavost Charpy-V – temperatura popuščanja. Iz izdelanih diagramov popuščanja lahko ugotovimo, da je preiskovano vzmetno jeklo 51CrV4 primerno za izdelavo visokotrdnostnih vzmeti ob ustrezno izvedeni toplotni obdelavi. Med fraktografsko in metalografsko analizo K_{Ic} preizkušancev smo odkrili prisotnost izcej v jeklu. Zato smo se posvetili ugotavljanju vpliva izcejanja na lomno žilavost K_{Ic}. Ugotovili smo, da se širina trakov pozitivnih izcej in trakov matriksa pri različnih vzorcih precej razlikuje. Prav tako smo odkrili, da število in širina izcej zaradi prisotnosti bainita v matriksu pomembno vplivata na lomno žilavost K_{Ic}.

Ključne besede: lomna žilavost, izcejanje, visokotrdnostno vzmetno jeklo, vakuumska toplotna obdelava, diagrami popuščanja, mikrostruktura

1 INTRODUCTION

A producer of spring steel must provide a technical description of the steel, which includes the chemical composition and the basic mechanical, physical and technological properties of the steel. Among the technological properties, information concerning the heat treatment is very important for the manufacturer of the springs.

Charpy-V notch (CVN) impact-test values are used in toughness specifications for spring steels, even though the fracturing energy is not directly related to the spring design. It is surprising that there is no demand for the fracture toughness K_{Ic} value (the plain-strain stress-intensity factor at the onset of unstable crack growth) in the delivery conditions for spring-steel producers. To the spring designer the K_{Ic} values are more useful than the CVN values, because the design calculations for the springs from high-strength steels should also take into account the strength and the toughness of the materials in order to prevent rapid and brittle fracture.

A spring's durability is limited by the plastic deformation, the fatigue and the fracturing. Therefore, the use of spring steel with the following properties is recommended: high ductility and toughness at operating temperatures from –40 °C to +50 °C and good hardenability, which provides the required mechanical properties. As a consequence of the manufacturing route, steels with a similar chemical composition may behave differently due to the variety of mechanical properties. Assuming that the chemical composition and initial microstructure of the steel correspond to those prescribed for the steel grade 51CrV4 (DIN 17221 and DIN 17222), the mechanical properties for a specific application depend mainly on the appropriately selected heat-treatment parameters.

An investigation was conducted to determine whether standardized fracture-toughness testing (ASTM E399-90), which is difficult to perform reliably for hard and low-ductility materials, could be replaced with a non-standard testing method using circumferentially notched and fatigue-precracked tensile specimens. The aim of this innovative investigation approach was to enable us to draw, for the normally used range of working hardness, combined tempering diagrams (Rockwell-C hardness – fracture toughness K_{Ic} – tempering temperature) for the vacuum-heat-treated high-strength spring-steel grade 51CrV4.

In addition, we also wanted to create, for the spring steel 51CrV4, at a selected austenitizing temperature, a classic tempering diagram, i.e., tensile strength R_m – yield stress $R_{p0.2}$ – elongation A_5 – necking Z – tempering temperature, and a tempering diagram, i.e., hardness HRc – impact toughness Charpy-V – tempering temperature. Using these tempering diagrams we wanted to confirm the suitability of the investigated steel for the production of high-strength springs with the required tensile strength between 1500 MPa and 1800 MPa.

In accordance with the plan of experiments the heat treatment was carried out on the basis of trial preliminary research and modelling results by measurements of the mechanical properties, analysis of the fractured surfaces and the examination of the microstructure of the K_{Ic} samples. Then, based on the mechanical properties the tempering diagrams for the spring steel 51CrV4, at a selected austenitizing temperature, were created.

Fractographic and metallographic analyses of the K_{Ic} test specimens showed the presence of segregations in the steel. Therefore, we also focused on examining the impact of segregations on the fracture toughness K_{Ic}. Using optical and electron (SEM + EDS) microscopy we determined the number and the width of the positive segregations bands and of the matrix bands just under the fractured surface of the K_{Ic} test specimens. We studied the influence of the number and the width of the segregation bands on the fracture toughness K_{Ic}.

2 EXPERIMENTAL

2.1 Hardness and fracture-toughness tests

Circumferentially notched and fatigue-precracked tensile-test specimens[1] with the dimensions indicated in **Figure 1** were used for the investigation. The Rockwell-C hardness (HRc) was measured on individual groups of K_{Ic} test specimens using a Wilson 4JR hardness machine.

The advantage of the K_{Ic} test specimens used here over standardized CT specimens (ASTM E399-90) is in the radial symmetry, which makes them particularly suitable for studying the influence of the microstructure of metallic materials on the fracture toughness. The advantage of these specimens is related to the heat transfer, which ensures a uniform microstructure.

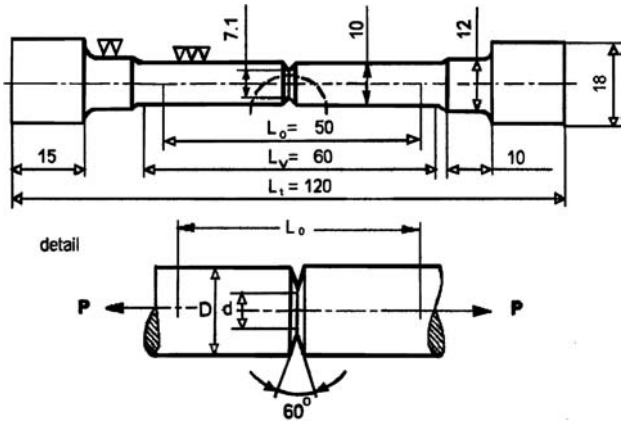

Figure 1: Circumferentially notched and fatigue-precracked K_{Ic} test specimen. Dimensions in mm.

Slika 1: Cilindrični natezni preizkušanec za merjenje lomne žilavosti z zarezo po obodu in utrujenostno razpoko v dnu zareze. Dimenzije so v milimetrih.

Due to the high notch sensitivity of hard and brittle metallic materials, such as continuous-cast spring-steel grade 51CrV4, it is very difficult – sometimes even almost impossible – to create a fatigue crack in the test specimen. However, with the K_{Ic} test specimens the fatigue crack can be created with rotating-bending loading before the final heat treatment[2]. The second advantage of such test specimens is that plain-strain conditions can be achieved using specimens with smaller dimensions than those of conventional CT test specimens[3].

For the linear elastic behaviour up to fracture of such specimens[4] the following equation is applied:

$$K_{Ic} = \frac{P}{D^{3/2}}\left(-1.27+1.72\frac{D}{d}\right) \quad (1)$$

where P is the load at failure, D is the outside diameter, and d is the notched-section diameter of the test specimen. Equation (1) is valid as long as the condition $0.5 < d/D < 0.8$ is fulfilled.

The measurements of the fracture toughness were performed at room temperature using an Instron 1255 tensile-test machine. A cross-head speed of 1.0 mm/min was used for the standard tensile tests on specimens with a nominal test length of 100 mm. In the tests two specially prepared cardan fixed jaws, ensuring the axiality of the tensile load, were used. During the tests the tensile-load/displacement relationship until failure was recorded. In all cases this relationship was linear, and the validity of equation (1) for the tests was confirmed.

2.2 Impact test

In order to obtain the tempering diagram, i.e., hardness HRc – Charpy-V – tempering temperature, we

measured the impact toughness using the Charpy impact test, known also as the Charpy V-notch test (ISO 148). The measurement with an instrumented Charpy hammer allows us to estimate the total impact work, the work needed for crack initiation and the work necessary for crack propagation.

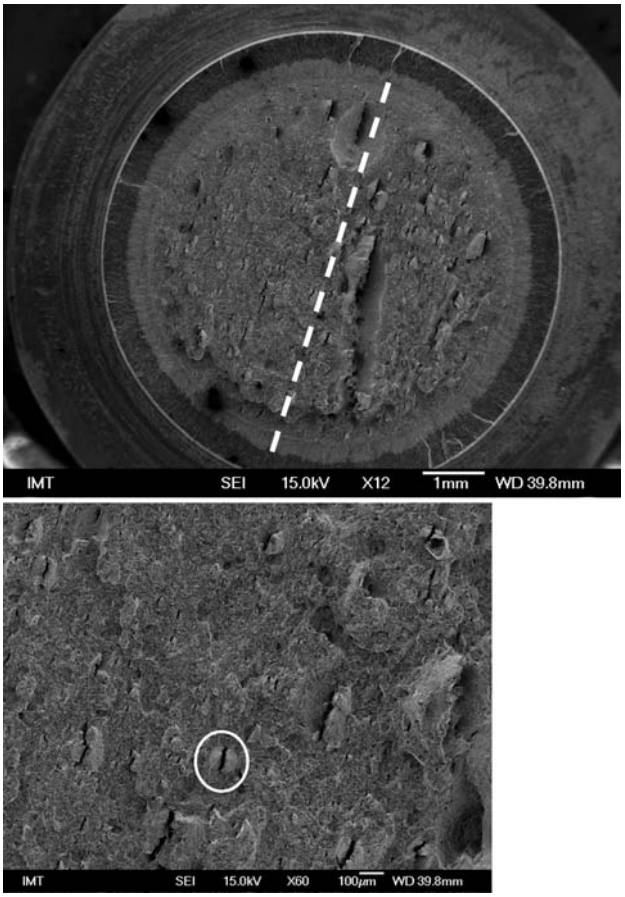

Figure 2: SEM image of fractured surface of K_{Ic} specimen
Slika 2: SEM posnetek prelomne površine preizkušanca za merjenje lomne žilavosti

The hardness HRc was measured on an Instron B 2000 device according to the standard SIST EN ISO 6508-1.

2.3 Tensile test

The standard tensile test (SIST EN ISO 6892-1) was applied to measure the tensile strength R_m, the yield stress $R_{p0.2}$, the elongation A_5 and the necking Z.

2.4 Material, sampling and vacuum heat treatment

Samples from continuous-cast, high-strength, spring-steel, grade 51CrV4, delivered as hot-rolled and soft-annealed bars of dimensions 100 mm × 25 mm × 6000 mm were used.

The circumferentially notched and fatigue-precracked K_{Ic} test specimens were cut from the middle of the bar in the rolling direction with a fatigue crack at the notch root in the transverse direction. They were heat treated in a horizontal vacuum furnace with uniform, high-pressure gas-quenching using nitrogen (N_2) at a pressure of 5 bar. After the first preheat (650 °C) the specimens were heated at a rate of 10 °C/min to the austenitizing temperature of 870 °C, soaked for 10 min, gas quenched to 80 °C, and then single tempered for one hour at different temperatures between 200 °C and 575 °C. At each tempering temperature 16 test specimens for the tensile test (R_m specimen), for the determination of the fracture toughness (K_{Ic} specimen) and of the Charpy-V toughness (CVN specimen), as well as two metallographic samples ϕ 19 mm × 9 mm were heat treated.

2.5 Measurement of the number and the width of the segregations

A fractured surface of a K_{Ic} specimen was observed on the SEM, **Figure 2**. The dotted line shows the orientation of the MnS sulphides. An example of the MnS inclusion inside the crack is shown in the circle.

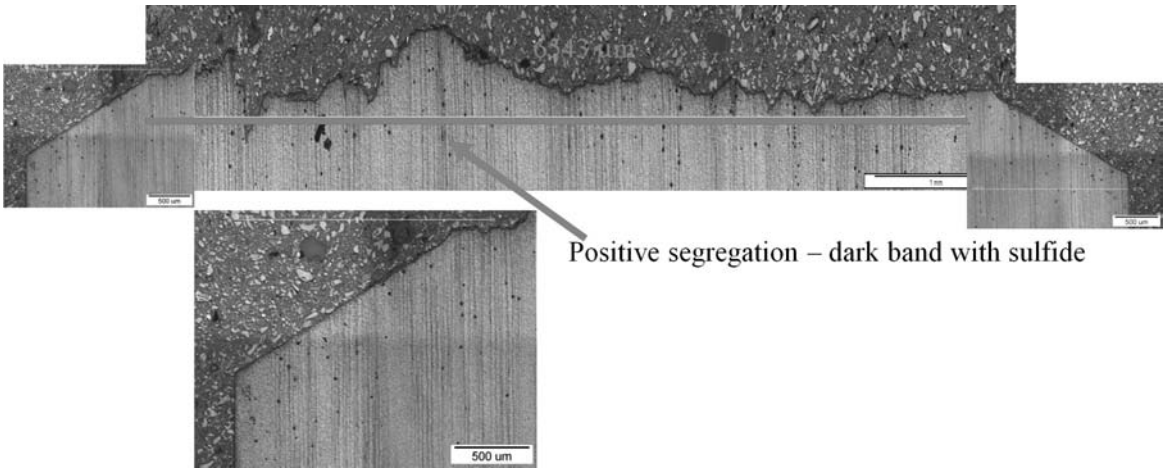

Figure 3: Combined image of segregations just under the fractured surface
Slika 3: Sestavljena slika izcej tik pod prelomno površino

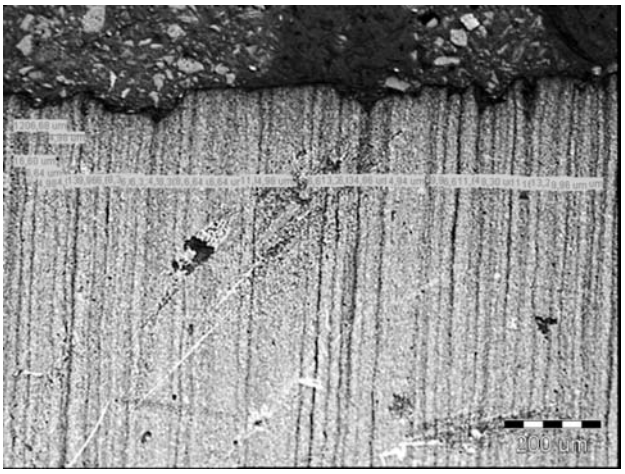

Figure 4: Microstructure of test specimen D99: positive segregations – tempered martensite (dark bands), 4% picral

Slika 4: Mikrostruktura preizkušanca D99: pozitivne izceje – popuščeni martenzit (temni pasovi), 4 % pikral

The presence of MnS in the crack was confirmed by EDS. Inclusions of MnS are present in positive segregations that are oriented in the rolling direction. To determine the number of segregations the K_{Ic} specimens were cut perpendicularly to the orientation of the MnS sulphides.

The number of segregations just under the fractured surface was counted using an optical microscope, as shown in **Figure 3**, on a sample etched in 4 % picral to make the segregations visible. The dark bands as positive segregations were confirmed by the presence of sulphides and by measuring the microhardness.

The assessment of the number and the width of the segregations is shown in **Figure 4**.

3 RESULTS AND DISCUSSION

In a classic tempering diagram for an austenitizing temperature of 870 °C the average measured values of the mechanical properties (tensile strength R_m/MPa, yield strength $R_{p0.2}$/MPa, elongation A_5/% and necking Z/%) are shown as a function of the tempering temperature in the range between 300 °C and 700 °C in **Figure 5**.

Given that we had for each selected tempering temperature a statistically relevant number of R_m specimens, for each group we performed a statistical analysis. As can be seen from the diagram, the minimum dispersion of results is within $\pm 2\sigma$ across the whole range of selected tempering temperatures in tensile strength and elongation, while it is higher only for the necking.

The tempering diagram indicates that the requirement from the standard DIN EN 10089:2003-4 for the elongation (minimum 8 %) and necking (minimum 30 %) can be achieved after the tempering of the investigated steel in the temperature range between 300 °C and 700 °C, while the required tensile strength (1350–1650 MPa) and

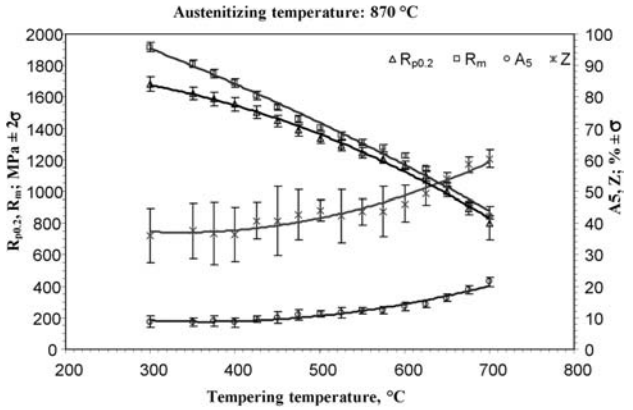

Figure 5: Classic tempering diagram for continuous-cast, hot-rolled, flat, spring steel 51CrV4, for an austenitizing temperature of 870 °C

Slika 5: Klasični diagram popuščanja za kontinuirno lito, vroče valjano vzmetno jeklo 51CrV4, temperatura avstenitizacije 870 °C

yield-strength (minimum 1200 MPa) can be achieved with a tempering temperature below 530 °C.

The required tensile strength for high-strength spring steel (1500–1800 MPa) can be achieved if the tempering temperature is below 475 °C.

The tempering diagram, hardness HRc – Charpy-V – tempering temperature, for the selected austenitizing temperature of 870 °C and the selected tempering temperature in the range of 200 °C to 625 °C for the high-strength steel 51CrV4 is shown in **Figure 6**. The diagram shows that the curves for the hardness and impact toughness Charpy-V over the entire range of tempering temperatures are similar to the curves of the hardness and the fracture toughness K_{Ic} in the tempering diagram shown in **Figure 7**. Similar to the fracture toughness, the impact toughness Charpy-V also increases to a temperature of 525 °C, then it decreases to 550 °C, and then the toughness increases again. This trend can be attributed to the kinetics of precipitation

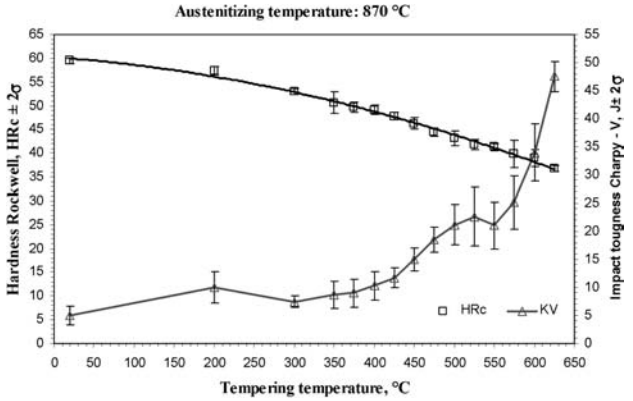

Figure 6: Effect of tempering temperature on the hardness HRc and the impact toughness Charpy-V of a continuous-cast, hot-rolled, flat, spring steel 51CrV4

Slika 6: Vpliv temperature popuščanja na trdoto HRc in udarno žilavost Charpy-V za kontinuirno lito, vroče valjano vzmetno jeklo 51CrV4

during the tempering. In the diagram, the dispersion of results within ±2σ in the quenched and tempered condition using a temperature of 475 °C is of the same magnitude. The dispersion of results is increased above the tempering temperature of 500 °C. The results of the measurements of the Charpy-V toughness in the range of tempering temperature 525–575 °C show that the toughness is even reduced, which confirms the observations made when measuring the fracture toughness, so we assume that this is an area of irreversible temper embrittlement[5,6].

In the case of the CVN-specimens, which were quenched and tempered at the same temperature, the reason for the scattering of the results is the heterogeneity of the investigated steel and also, but less of a factor, the geometry and surface roughness of the notch.

The requirement from the standard DIN EN 10089: 2003-04 for the impact energy (minimum 8 %) can be achieved if the tempering temperature is above 200 °C.

High-strength spring steels are very notch sensitive, for this occasion, it is also important to measure fracture toughness K_{Ic}, which can be described as the ability of a material to resist, under tensile loading, the progress of existing cracks. We determined the fracture toughness K_{Ic} by the use of circumferentially notched and fatigue-precracked K_{Ic} test specimens which were linear elastic loaded to fracture. The tempering diagram, hardness HRc – fracture toughness K_{Ic} – tempering temperature, for the selected austenitizing temperature of 870 °C and the selected tempering temperature in the range of 200 °C to 625 °C for the steel 51CrV4 is shown in **Figure 7**.

Given that we had for each selected tempering temperature a statistically relevant number of K_{Ic} specimens, for each group we performed a statistical analysis. As can be seen from the diagram, the minimum dispersion of results within ±2 s is in the quenched state and in K_{Ic} specimens that were quenched and tempered at 200 °C. At higher tempering temperatures between 300 °C and 525 °C, the scattering of the results slightly increased. This trend can be attributed to the kinetics of extracting precipitates during tempering. The reason for the dispersion of the results within each group of K_{Ic} specimens that were quenched and tempered at the same temperature is the heterogeneity of the investigated steel.

The highest hardness of 58 HRc is achieved in the as-quenched condition after vacuum quenching from the austenitizing temperature of 870 °C. In examining the evolution of the properties by an increase of the tempering temperatures, it is observed that the minimum scatter of results within ± 2σ = 3.2 MPa m$^{1/2}$ is found in the as-quenched state and after single tempering at 200 °C. At higher tempering temperatures between 300 °C and 575 °C, the scatter of the K_{Ic} results slightly increased up to ±2σ = 9.4 MPa m$^{1/2}$, while the scatter of the Rockwell-C hardness is up to ±2σ = 1.2 HRc across the whole range of used tempering temperatures. Within each group of K_{Ic} specimens that were quenched and tempered at the same temperature, this can be attributed to the kinetics of the carbides' precipitation during tempering at selected temperatures as well as to the

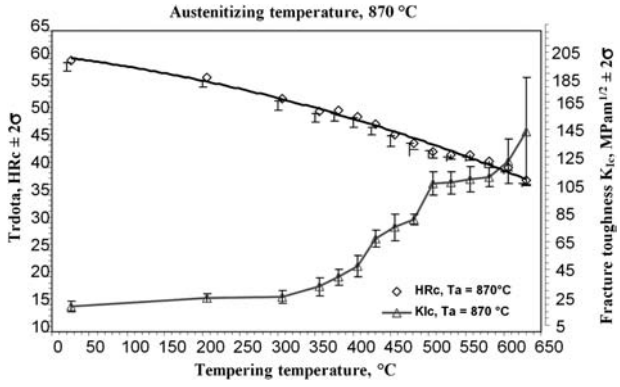

Figure 7: Effect of tempering temperature on the hardness HRc and the fracture toughness K_{Ic} of the continuous-cast, hot-rolled, flat, spring steel 51CrV4

Slika 7: Vpliv temperature popuščanja na trdoto HRc in lomno žilavost K_{Ic} za kontinuirno lito, vroče valjano vzmetno jeklo 51CrV4

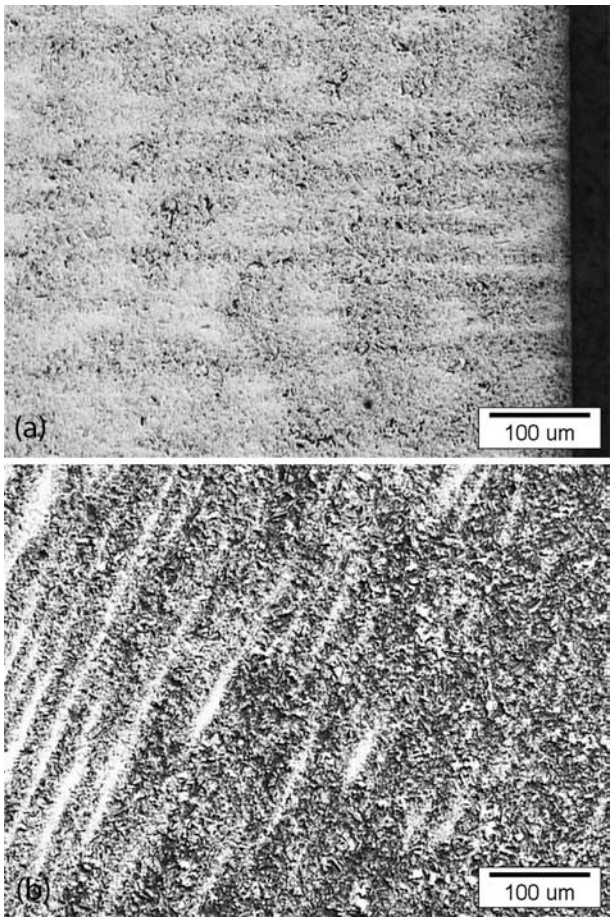

Figure 8: The microstructure of the K_{Ic} test specimen in the as-quenched condition (transverse direction); a) specimen with the lowest fracture toughness (K_{Ic}= 16.2 MPa m$^{1/2}$, 58.1 HRc), b) specimen with the highest fracture toughness (K_{Ic}= 22.3 MPa m$^{1/2}$, 58.1 HRc)

Slika 8: Mikrostruktura K_{Ic} preizkušanca v kaljenem stanju (prečna smer); a) z najmanjšo lomno žilavostjo (K_{Ic}= 16,2 MPa m$^{1/2}$, 58,1 HRc), b) z največjo lomno žilavostjo (K_{Ic}= 22,3 MPa m$^{1/2}$, 58,1 HRc)

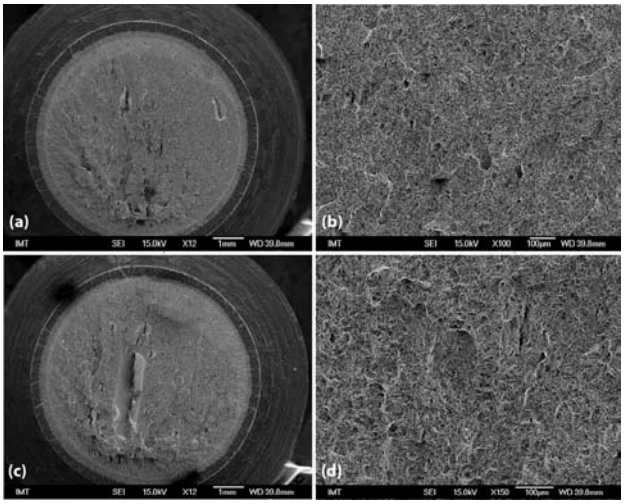

Figure 9: Fractured surfaces of K_{Ic} test specimen, tempered at 475 °C with an equal hardness; a, b) specimen with the lowest fracture toughness (K_{Ic} = 67.0 MPa $m^{1/2}$, 44.8 HRc), c, d) specimen with the highest fracture toughness (K_{Ic} = 76.1 MPa $m^{1/2}$ in 44.8 HRc)

Slika 9: Prelomne površine K_{Ic} preizkušancev popuščenih pri 475 °C z enako trdoto; a, b) z najmanjšo lomno žilavostjo (K_{Ic} = 67,0 MPa $m^{1/2}$, 44,8 HRc), c, d) z največjo lomno žilavostjo (K_{Ic} = 76,1 MPa $m^{1/2}$ in 44,8 HRc)

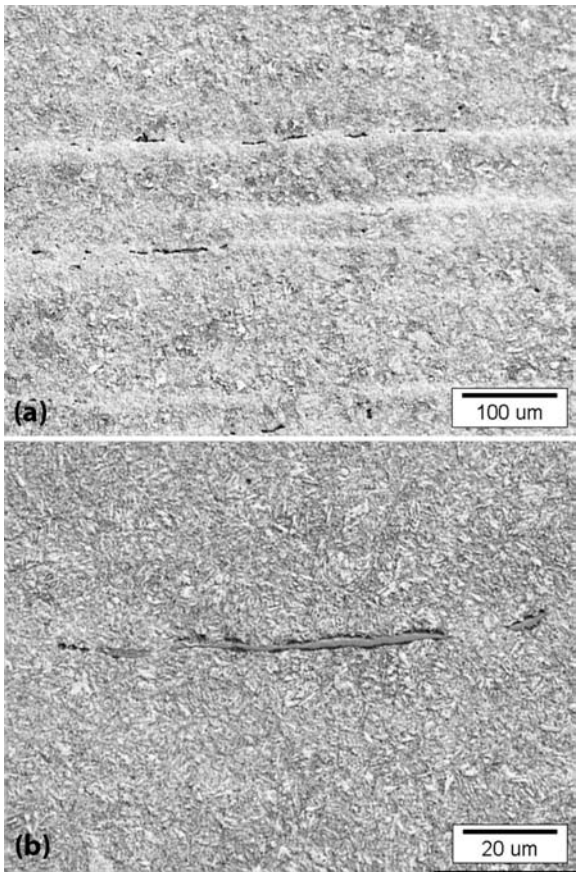

Figure 10: Typical microstructure of K_{Ic} test specimens (K_{Ic} = 75.7 MPa $m^{1/2}$, 43.8 HRc) in the longitudinal direction. Sulphide inclusions are located in the positive segregations.

Slika 10: Značilna mikrostruktura K_{Ic} preizkušanca (K_{Ic} = 75,7 MPa $m^{1/2}$, 43,8 HRc) v vzdolžni smeri. Sulfidi se nahajajo v pozitivnih izcejah.

heterogeneity of the investigated steel. Since the austenitizing temperature is the same, it is clear that the fracture toughness, K_{Ic}, is a very selective mechanical property with regard to the tempering temperature. It should be noted that the K_{Ic} test specimens were taken from the middle of the bar, and therefore the microstructures of the K_{Ic} test specimens with lowest and highest fracture toughnesses are comparable.

In the as-quenched condition, the microstructure consists of untempered martensite and lower bainite, **Figure 8**. Strong positive (bright) and negative (dark) segregations are visible due to the lower etching intensity of the untempered martensite.

The fractured surface of the K_{Ic} test specimens was examined in SEM at magnification of 12-times, **Figure 9**. The presence of inclusions (sulphides in cracks) in positive segregations is evident. The density of positive segregations is higher on the fractured surface of the K_{Ic} test specimen with the highest fracture toughness in comparison to the fractured surface of the K_{Ic} test specimen with the lowest fracture toughness with the

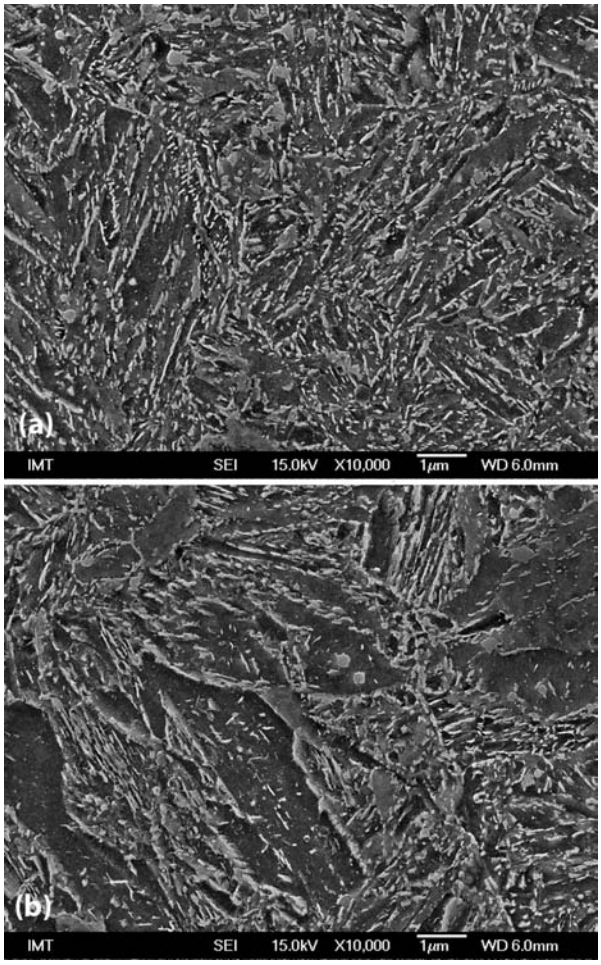

Figure 11: SEM microstructure of the K_{Ic} test specimens with the highest fracture toughness: a) positive segregations and b) negative segregations (matrix), longitudinal direction

Slika 11: SEM-mikrostrukture K_{Ic} preizkušanca z največjo lomno žilavostjo: a) pozitivna izceja, b) negativna izceja, vzdolžna smer

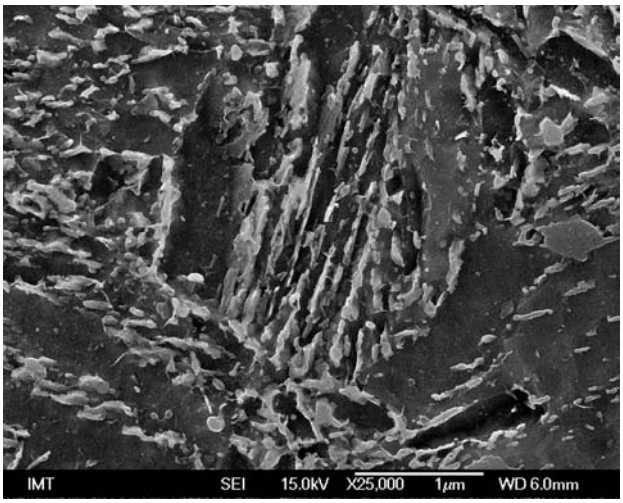

Figure 12: Bainite grain from **Figure 11**
Slika 12: Kristalno zrno bainita s **slike 11**

same hardness. Also, the distribution is more even and the size of the segregations is smaller.

The microstructure of the same K_{Ic} specimens just below the fractured surface was examined in an optical microscope, **Figure 10**. The fractured K_{Ic} specimen was cut perpendicularly to the direction of segregations determined by the position of the sulphide inclusions. Then the number of segregations in the transverse direction was counted and for the specimen with the lowest fracture toughness (K_{Ic} = 67.0 MPa m$^{1/2}$, 44.8 HRc) 98 segregations and specimen with the highest fracture toughness (K_{Ic} = 76.1 MPa m$^{1/2}$, 44.8 HRc) 147 segregations were found. We also measured the widths of the segregation bands. The specimen with the lowest fracture toughness has an average width of the segregation bands equal to 29 μm and that with the highest fracture toughness has an average width of the segregation bands equal to 33 μm.

The microstructure in the quenched and tempered condition consists of tempered martensite and bainite (≈20 %, volume fraction). In the microstructure, non-metallic inclusions of the sulphide type located in positive segregations and oriented in the rolling direction are observed.

The microstructure of the K_{Ic} test specimen was examined in the SEM and it was found that the microstructure in the positive segregations consisted of tempered martensite and in the negative (matrix) of tempered martensite with islands of bainite, **Figures 11** and **12**.

From a comparison of the microstructures of the K_{Ic} test specimens with the lowest and highest fracture toughnesses from the same heat and with the same hardness, it can be concluded that the density, the size and the distribution of segregations have a significant influence on the fracture toughness. The increase of

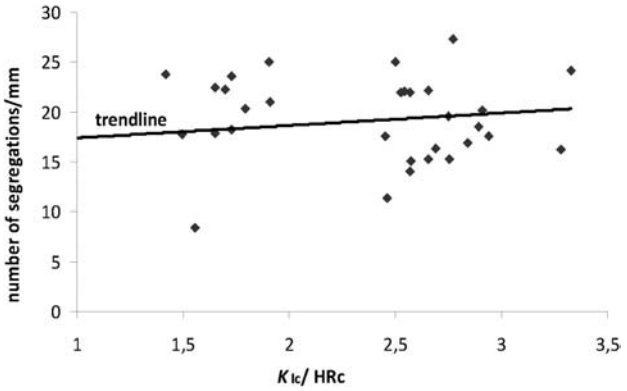

Figure 13: Influence of the number of segregations on the fracture toughness K_{Ic}
Slika 13: Vpliv števila izcej na lomno žilavost K_{Ic}

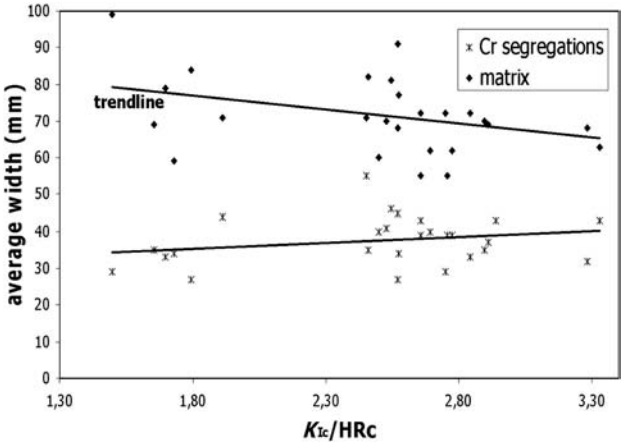

Figure 14: Influence of the average width of the matrix bands and the segregation bands on the fracture toughness K_{Ic}
Slika 14: Vpliv povprečne širine pasov negativnih in pozitivnih izcej na lomno žilavost K_{Ic}

fracture toughness can probably be ascribed to the presence of bainite in the matrix of negative segregations.

To find out the influence of segregation on the fracture toughness the number of segregations and their width just under the fractured surface were assessed, **Figures 13** and **14**.

It can be seen that there is a trend for the fracture toughness K_{Ic} to increase with a larger number of segregations. It is also evident that the average width of the segregations affects the fracture toughness K_{Ic}. The broad bands of the positive segregations increase the fracture toughness K_{Ic}, while it is lowered by narrow bands of the matrix. This can also be associated with the number of segregations. If there are more segregations, the average width of the matrix bands decreases.

4 CONCLUSIONS

The investigated high-strength, spring-steel grade 51CrV4 was successfully quenched in a horizontal vacuum furnace with uniform high-pressure gas-quench-

ing using nitrogen (N_2) at a pressure of 5 bar. The Rockwell-C hardness was (58.4 ± 0.8) HRc in the quenched state, which is high enough to obtain the required hardnesses from 35 HRc to 50 HRc after a single tempering.

The obtained microstructure consisting of tempered martensite and bainite (≈20 % volume fraction) meets the requirements of TB1402 (Scania Standard STD512090 and STD4153), thus we can conclude that the investigated high-strength spring steel 51CrV4 with a thickness up to 20 mm is suitable for heat treatment in a vacuum furnace with uniform, high-pressure gas-quenching using nitrogen (N_2) at a pressure of 5 bar or higher.

Our investigation showed that standardized fracture-toughness testing (ASTM E399-90) could be replaced with a non-standard testing method using circumferentially notched and fatigue-precracked tensile specimens (K_{Ic} test specimen). The results of this innovative approach to the investigation have shown that using the proposed method it was possible to draw, for the normally used range of working hardness, combined tempering diagrams (Rockwell-C hardness – Fracture toughness K_{Ic} – Tempering temperature) for vacuum-heat-treated, high-strength, spring-steel grade 51CrV4.

According to the tempering diagrams the tensile strength R_m – Yield stress $R_{p0.2}$ – Elongation A_5 – Necking Z – Tempering temperature and the tempering diagram, Hardness HRc – Impact toughness Charpy-V – Tempering temperature, we can conclude that the investigated spring steel 51CrV4 is suitable for the production of high-strength springs when the proper heat treatment is performed.

The presence of segregations was confirmed by fractographic and metallographic analyses of the K_{Ic} test specimens. We found that the width of the positive segregation bands and matrix bands between the samples varied considerably. We have also discovered that the number and the width of the segregation bands influenced significantly the fracture toughness K_{Ic} due to the presence of bainite in the matrix bands. Our investigation shows that there is a trend of fracture toughness K_{Ic} increase with a larger number of segregations.

These findings will be checked in future investigations.

Acknowledgement

Štore Steel, d. o. o., Železarska 3, SI-3220 Štore, Slovenia, is thanked for the supply of test material as well for the financial support. Thanks also to Prof. dr. Franc Vodopivec for helpful discussions.

5 REFERENCES

[1] B. Senčič, V. Leskovšek, Mater. Tehnol., 45 (**2011**) 1, 67–73

[2] A. Sandberg, M. Nzotta, High performance matrix tool steels produced via a clean steel concept, 7th Tooling Conference, Torino, 2006

[3] V. Leskovšek, Optimization of the vacuum heat treatment of high-speed steels, University of Zagreb, 1999 (Ph. D. thesis)

[4] H. F. Bueckner, ASTM STP 381, 1965, 82

[5] A. Shekhter, S. Kim, D. G. Carr, A. B. L. Croker, S. P. Ringer, International Journal of Pressure Vessels and Piping, 79 (**2002**), 611–615

[6] B. Ule, F. Vodopivec, M. Pristavec, F. Grešovnik, Železarski zbornik, 24 (**1990**), 35–40